Acta Mechanica 125, 17–30 (1997)

ACTA MECHANICA

Flexural vibrations of elastic composite beams with interlayer slip

C. Adam, R. Heuer, and **A. Jeschko,** Vienna, Austria

Dedicated to Prof. Dr. Dr. h. c. Franz Ziegler on the occasion of his 60th birthday

(Received April 30, 1997)

Summary. The objective of the present paper is to analyze the dynamic flexural behavior of elastic two-layer beams with interlayer slip. The Bernoulli-Euler hypothesis is assumed to hold for each layer separately, and a linear constitutive equation between the horizontal slip and the interlaminar shear force is considered. The governing sixth-order initial-boundary value problem is solved by separating the dynamic response in a quasistatic and in a complementary dynamic response. The quasistatic portion that may also contain singularities or discontinuities due to sudden load changes is determined in a closed form. The remaining complementary dynamic part is non-singular and can be approximated by a truncated modal series of fast accelerated convergence. The solution of the resulting generalized decoupled single-degree-of-freedom oscillators is given by means of Duhamel,s convolution integral, whereby the velocity and acceleration of the loads are the driving terms. Light damping is considered via modal damping coefficients. The proposed procedure is illustrated for dynamically loaded layered single-span beams with interlayer slip, and the improvement in comparison to the classical modal analysis is demonstrated.

1 Introduction

Layered structures are designed for engineering applications where both high strength-to-weight and stiffness-to-weight ratios are required. Due to modern technologies, a problem-oriented choice of the material properties in different layers becomes possible [1]. If the layers are connected continuously by means of strong adhesives, the mechanical assumption of a rigid interconnection between the layers is reasonable. In the last four decades various types of classical as well as higher order linear elastic composite theories for perfectly bonded beams, plates, and shells have been developed, where basically two classes of theories can be distinguished: the equivalent-single-layer theories and the layerwise laminate theories, compare [2]. The latter category is derived by admitting a separate displacement field within the individual layers of the composite, see [3]–[5]. Besides the equations of motion an additional set of equations is obtained by prescribing the continuity of the transverse shear stresses across the interfaces. Alternatively, the extension of homogeneous beam and plate theories is based on one displacement expansion throughout the thickness of the laminate that results in equivalent-single-layer theories, e.g. [6], [7]. Consequently, the transverse strains are continuous through the laminate thickness. Such theories cannot accurately model laminates made of dissimilar materials layers.

In some widely used structures, such as in composite steel-concrete beams or in layered wood systems connected with nails, rigid bond between the layers cannot be achieved. Due to relative deformation of the connectors an interlayer slip occurs, that significantly can affect both strength and deformation of the layered structure. Linear static analysis of layered beams with partial or

flexible connection is well established in [8]–[12]. An extension to steel and concrete composite beams with nonlinear shear force-slip relationship is introduced in [13].

The present paper is concerned with the dynamic analysis of two-layer composite beams with linear elastic interlayer slip. In case of dynamic loading, the partial interaction also increases the damping capacity of the structure. Girhammar and Pan [14] solve the governing boundary value problem by modal analysis, where the deflection is transformed to a set of modal amplitudes. This procedure leads to solutions which are slowly convergent or even divergent. Hence, this paper introduces a different approach. Thereby, the dynamic response is separated in a quasistatic and in a complementary dynamic response, and a modal expansion is performed only for the complementary dynamic part of the solution. The quasistatic portion is determined separately and in a closed form by means of weighted integration of the corresponding influence function. Such a splitting is numerically efficient and also more accurate since the quasistatic part may contain singularities or discontinuities that are properly accounted for and which would be poorly modeled by a truncated modal series solution. The remaining complementary dynamic response is non-singular and can be approximated by a finite modal series of fast accelerated convergence. This type of solution procedure has been first suggested by Boley and Barber [15] for the analysis of rapidly heated beams and plates and was later picked up by Ziegler et al. ([16]–[21]), in order to analyze the elastic-plastic behavior of beams and plates. An additional convenient feature of that kind of modal approach is the incorporation of viscous damping, that is introduced via modal damping coefficients. The proposed procedure is illustrated for simply supported two-layer beams with interlayer slip for various loading functions, and the improvement in comparison to the classical modal analysis is shown.

2 Governing equations for two-layer beams with interlayer slip

Plane bending of two-layer composite beams with partial interaction is inspected. Due to an interlayer slip considered between the layers, the Bernoulli-Euler hypothesis is not applicable for the cross-section as a whole. However, the assumption that plane sections remain plane after deformation is still valid for each individual layer. In case of composite elements with concentrated mechanical shear connections like bolts and nails, it is assumed that the concentrated slip forces are distributed uniformly along the length of the member. Since the interlaminar slip Δu is assumed to be a linear function of the shear force T transmitted between the two layers, the slip is given by

$$\Delta u = \frac{T}{k}, \tag{1}$$

where k is a constant slip modulus.

The equation of flexural motion is derived by considering the free-body diagram of an infinitesimal beam element with distributed transverse force q. Application of the conservation of momentum in transverse direction renders together with Eq. (1) the following partial differential equation of motion for the lateral deflection w ([14]):

$$w_{,xxxxxx} - \alpha^2 w_{,xxxx} + \frac{\mu}{EJ_0}\ddot{w}_{,xx} - \alpha^2 \frac{\mu}{EJ_\infty}\ddot{w} = -\frac{\alpha^2}{EJ_\infty} q + \frac{1}{EJ_0} q_{,xx}. \tag{2}$$

x represents the axial beam coordinate, and $()_{,x}$ and $\dot{()}$ stand for the spatial and time derivatives. μ denotes the mass per unit length,

$$\mu = \varrho_1 A_1 + \varrho_2 A_2, \tag{3}$$

EJ_0 and EJ_∞ are the bending stiffness corresponding to non-composite actions (subscript 0) and to a rigid interlayer connection (subscript ∞), respectively,

$$EJ_0 = E_1J_1 + E_2J_2, \qquad EJ_\infty = EJ_0 + \frac{EA_pr^2}{EA_0}. \tag{4}$$

EA_0 identifies the longitudinal stiffness,

$$EA_0 = E_1A_1 + E_2A_2, \tag{5}$$

and the abbreviations α^2 and EA_p are defined as

$$\alpha^2 = k\left(\frac{EA_0}{EA_p} + \frac{r^2}{EJ_0}\right), \qquad EA_p = E_1A_1E_2A_2. \tag{6}$$

In Eqs. (2)–(6), ϱ_i, A_i, E_i denote the mass densities, cross-sectional areas and Young's moduli of the individual layers, respectively, J_i are the principle moments of inertia of each cross-sectional area, and r represents the vertical distance between the centers of gravity of the two layers, see Fig. 1.

The solution of Eq. (2) depends on the initial conditions at time instant $t = 0$ and on the actual boundary conditions at point x_b. In the following, three classical boundary conditions are summarized, compare [14]:

(i) Simply supported end:

$$w(x_b, t) = 0, \qquad M_i(x_b, t) = 0, \qquad N_1(x_b, t) = 0, \tag{7.1}$$

or when expressed through w and its derivatives,

$$w(x_b, t) = 0, \qquad w_{,xx}(x_b, t) = 0, \qquad w_{,xxxx}(x_b, t) = \frac{q(x_b, t)}{EJ_0}. \tag{7.2}$$

(ii) Clamped end:

$$w(x_b, t) = 0, \qquad w_{,x}(x_b, t) = 0, \qquad \Delta u(x_b, t) = 0, \tag{8.1}$$

or

$$w(x_b, t) = 0, \qquad w_{,x}(x_b, t) = 0, \qquad w_{,xxxxx}(x_b, t) - \alpha^2\left(1 - \frac{EJ_0}{EJ_\infty}\right) w_{,xxx}(x_b, t) = \frac{q_{,x}(x_b, t)}{EJ_0}. \tag{8.2}$$

(iii) Free end:

$$M_i(x_b, t) = 0, \qquad N_1(x_b, t) = 0, \qquad Q(x_b, t) = 0, \tag{9.1}$$

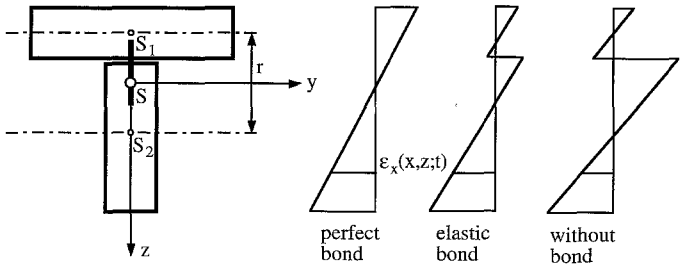

Fig. 1. Cross-section and horizontal strain distribution of two-layer beams with various interlaminar connection conditions

or

$$w_{,xx}(x_b,t)=0, \qquad w_{,xxxx}(x_b,t)+\frac{\mu}{EJ_0}\ddot{w}(x_b,t)=\frac{q(x_b,t)}{EJ_0},$$
$$w_{,xxxxx}(x_b,t)-\alpha^2 w_{,xxx}(x_b,t)+\frac{\mu}{EJ_0}\ddot{w}_{,x}(x_b,t)=\frac{q_{,x}(x_b,t)}{EJ_0}. \tag{9.2}$$

The bending moment M, the shear force Q, normal forces N_1, N_2 and the slip force per unit length T are determined following the lines of Jeschko [22]:

$$M=-EJ_\infty w_{,xx}+\frac{EJ_\infty}{\alpha^2}w_{,xxxx}-\frac{EJ_\infty}{\alpha^2 EJ_0}q, \tag{10.1}$$

$$Q=-EJ_\infty w_{,xxx}+\frac{EJ_\infty}{\alpha^2}w_{,xxxxx}-\frac{EJ_\infty}{\alpha^2 EJ_0}q_{,x}, \tag{10.2}$$

$$N_1=-N_2=-\frac{1}{r}\left[(EJ_0-EJ_\infty)w_{,xx}+\frac{EJ_\infty}{\alpha^2}w_{,xxxx}-\frac{EJ_\infty}{\alpha^2 EJ_0}q\right], \tag{10.3}$$

$$T=\frac{1}{r}\left[(EJ_0-EJ_\infty)w_{,xxx}+\frac{EJ_\infty}{\alpha^2}w_{,xxxxx}-\frac{EJ_\infty}{\alpha^2 EJ_0}q_{,x}\right]. \tag{10.4}$$

3 Dynamic response analysis

Within a linear theory of beam structures the quasistatic response can always be represented in a closed form. The quasistatic part of the solution possibly contains singularities or discontinuities, whereas the remaining dynamic part of the solution is non-singular. Due to its smooth behavior, this remaining part can be described by means of a relatively small number of eigenmodes. Consequently, the total response $w(x,t)$ will be formulated as the sum of its analytic quasistatic part (denoted by a subscript $()_S$) and a modal expansion of its complementary dynamic portion (denoted by a subscript $()_D$), ([15]–[21]),

$$w(x,t)=w_S(x,t)+w_D(x,t). \tag{11}$$

Replacing $w(x,t)$ of the partial differential equation (2) by the expression of Eq. (11) renders:

$$w_{S,xxxxxx}+w_{D,xxxxxx}-\alpha^2 w_{S,xxxx}-\alpha^2 w_{D,xxxx}+\frac{\mu}{EJ_0}\ddot{w}_{S,xx}+\frac{\mu}{EJ_0}\ddot{w}_{D,xx}$$
$$-\alpha^2\frac{\mu}{EJ_\infty}\ddot{w}_S-\alpha^2\frac{\mu}{EJ_\infty}\ddot{w}_D=-\frac{\alpha^2}{EJ_\infty}q+\frac{1}{EJ_0}q_{,xx}. \tag{12}$$

Considering the differential equation of the quasistatic deflection,

$$w_{S,xxxxxx}-\alpha^2 w_{S,xxxx}=-\frac{\alpha^2}{EJ_\infty}q+\frac{1}{EJ_0}q_{,xx}, \tag{13}$$

the equation of motion of the complementary dynamic response can be separated from Eq. (12):

$$w_{D,xxxxxx}-\alpha^2 w_{D,xxxx}+\frac{\mu}{EJ_0}\ddot{w}_{D,xx}-\alpha^2\frac{\mu}{EJ_\infty}\ddot{w}_D=\alpha^2\frac{\mu}{EJ_\infty}\ddot{w}_S-\frac{\mu}{EJ_0}\ddot{w}_{S,xx}. \tag{14}$$

The solution of Eq. (14) is found by modal analysis. Thereby, the quasistatic part w_S and the complementary dynamic portion w_D of the lateral deflection are transformed to a set of modal amplitudes. This transformation is expressed as

$$w_S(x,t) = \sum_{n=1}^{\infty} Y_n^S(t)\, \boldsymbol{\Phi}_n(x), \tag{15.1}$$

$$w_D(x,t) = \sum_{n=1}^{\infty} Y_n^D(t)\, \boldsymbol{\Phi}_n(x), \tag{15.2}$$

where $\boldsymbol{\Phi}_n$ stands for the mode shapes of the corresponding boundary value problem. The orthogonality relation of normalized mode shapes is given by (see [22])

$$\int_0^l \boldsymbol{\Phi}_n \left(-\frac{\mu}{EJ_0}\, \boldsymbol{\Phi}_{m,xx} + \alpha^2 \frac{\mu}{EJ_\infty}\, \boldsymbol{\Phi}_m \right) dx + \sum_{j=1}^{2} \boldsymbol{\Phi}_n(0,l)\, \boldsymbol{C}_j[\boldsymbol{\Phi}_m(0,l)] = \delta_{mn}, \tag{16}$$

where δ_{mn} is the Kronecker delta and $\boldsymbol{C}_j$ denotes a linear homogeneous differential operator containing derivatives of the boundaries as listed below.

(i) Simply supported or clamped end:

$$\boldsymbol{C}_1 = \boldsymbol{C}_2 = 0. \tag{17.1}$$

(ii) Free end:

$$\boldsymbol{C}_1 = \frac{\mu}{EJ_0}(), \qquad \boldsymbol{C}_2 = \frac{\mu}{EJ_0}()_{,x}. \tag{17.2}$$

The modal series Eqs. (15) are inserted into Eq. (14), multiplied by $\boldsymbol{\Phi}_m$, and integrated over the beam length l. Considering the orthogonality relations Eq. (16) leads to a formally uncoupled system of SDOF-oscillator equations for the complementary dynamic variables $Y_n^D(t)$:

$$\ddot{Y}_n^D + \omega_n^2 Y_n^D = -\ddot{Y}_n^S. \tag{18}$$

In the next step, Y_n^S is evaluated following the procedures of [22, p. 30] and [23, p. 391]: The boundary conditions Eqs. (9) are modified for the static case by neglecting the inertia terms and are added to Eq. (13). Inserting Eq. (15.1) into the resulting expression, multiplying by $\boldsymbol{\Phi}_m$, and integrating over length l, the quasistatic modal amplitudes become

$$Y_n^S(t) = \frac{1}{\omega_n^2} P_n(t), \tag{19}$$

where

$$P_n(t) = \int_0^l \boldsymbol{\Phi}_n \left[\frac{\alpha^2}{EJ_\infty}\, q - \frac{1}{EJ_0}\, q_{,xx} \right] dx + \sum_{j=1}^{2} \boldsymbol{\Phi}_n(0,l)\, \boldsymbol{C}_j[q(0,l)] \tag{20}$$

is the generalized loading associated with the mode shape $\boldsymbol{\Phi}_n$. Finally, the solution of Eq. (18) is given by means of Duhamel's convolution integral ([24]),

$$Y_n^D(t) = \frac{1}{\omega_n} \dot{Y}_n^D(0) \sin \omega_n t + Y_n^D(0) \cos \omega_n t - \frac{1}{\omega_n^3} \int_0^t \ddot{P}_n(\tau) \sin \omega_n (t-\tau)\, d\tau \tag{21}$$

where $Y_n^D(0)$, $\dot{Y}_n^D(0)$ represent the initial conditions.

4 Consideration of viscous damping

In the preceding formulations of equations of motion, no damping was included. However, in case of layered beams with elastic bond, the shear connectors also govern the energy absorption capacity and the damping characteristics. Within a linear theory this kind of distributed damping can be introduced directly into the modal equations of motion (18) via modal viscous damping coefficients ζ_n:

$$\ddot{Y}_n^D + 2\zeta_n\omega_n\dot{Y}_n^D + \omega_n^2 Y_n^D = -\ddot{Y}_n^S - 2\zeta_n\omega_n\dot{Y}_n^S. \tag{22}$$

Accordingly, each mode can be damped individually, which seems to be more general in comparison to introducing a stiffness- or/and mass-proportional Rayleigh damping into the partial differential equation (2). The solution of Eq. (22) is again given by Duhamel's convolution integral, whereby the undamped unit impulse response has to be replaced by the damped one, compare Ziegler [25]:

$$Y_n^D(t) = \exp(-\zeta_n\omega_n t)\left[(\cos\omega_{dn}t + \frac{\omega_n}{\omega_{dn}}\zeta_n \sin\omega_{dn}t)\, Y_n^D(0) + \frac{1}{\omega_{dn}}\sin\omega_{dn}t\,\dot{Y}_n^D(0)\right]$$

$$-\frac{1}{\omega_n^2}\frac{1}{\omega_{dn}}\int_0^t [\ddot{P}_n(\tau) + 2\zeta_n\omega_n\dot{P}_n(\tau)]\exp[-\zeta_n\omega_n(t-\tau)]\sin[\omega_{dn}(t-\tau)]\,d\tau. \tag{23}$$

In Eq. (23), ω_{dn} stands for the n-th eigenfrequency of the damped system,

$$\omega_{dn} = \omega_n\sqrt{1-\zeta_n^2} \approx \omega_n, \qquad \zeta_n \leq 0.2. \tag{24}$$

5 Numerical examples

The proposed procedure is applied to simply supported two-layer beams with partial interlaminar connection, see Fig. 2. The free response analysis renders the mode shapes

$$\boldsymbol{\Phi}_n(x) = A_n \sin\lambda_{1n}x, \qquad n = 1, 2, 3, \ldots, \tag{25}$$

with

$$\lambda_{1n} = \frac{n\pi}{l}, \qquad A_n = \left[\frac{\mu l}{2}\left(\frac{\alpha^2}{EJ_\infty} + \frac{\lambda_{1n}^2}{EJ_0}\right)\right]^{-1/2}, \tag{26}$$

and the corresponding eigenfrequencies, compare [14], [22],

$$\omega_n^2 = \lambda_{1n}^4(\lambda_{1n}^2 + \alpha^2)\left[\mu\left(\frac{\alpha^2}{EJ_\infty} + \frac{\lambda_{1n}^2}{EJ_0}\right)\right]^{-1}. \tag{27}$$

The quasistatic response w_S is evaluated most conveniently by means of the method of influence functions,

$$w_S(x,t) = \int_0^l \tilde{w}_S(\xi, x)\, q(\xi, t)\, d\xi, \tag{28}$$

where $\tilde{w}_S$ is the lateral deflection at point ξ produced by a single unit force applied in x. The static Green's function $\tilde{w}_S$ of the boundary value problem considered reads as follows:

$$\tilde{w}_S(\xi, x) = \frac{l^3}{6EJ_\infty}\left(1-\frac{x}{l}\right)\frac{\xi}{l}\left[1-\left(1-\frac{x}{l}\right)^2-\left(\frac{\xi}{l}\right)^2\right] + \frac{1}{\alpha^2}\left(\frac{1}{EJ_0}-\frac{1}{EJ_\infty}\right)\left[\frac{\sinh\alpha\xi\,\sinh\alpha(x-l)}{\alpha\sinh\alpha l}+\xi\left(1-\frac{x}{l}\right)\right], \qquad \xi \le x, \tag{29.1}$$

$$\tilde{w}_S(\xi, x) = \frac{l^3}{6EJ_\infty}\left(1-\frac{\xi}{l}\right)\frac{x}{l}\left[1-\left(\frac{x}{l}\right)^2-\left(1-\frac{\xi}{l}\right)^2\right] + \frac{1}{\alpha^2}\left(\frac{1}{EJ_0}-\frac{1}{EJ_\infty}\right)\left[\frac{\sinh\alpha(\xi-l)\,\sinh\alpha x}{\alpha\sinh\alpha l}+x\left(1-\frac{\xi}{l}\right)\right], \qquad \xi \ge x. \tag{29.2}$$

Only the complementary dynamic deflection $w_D(x,t)$ has to be determined by the modal expansion, Eq. (15.2).

In the following examples, the results obtained by the proposed procedure are compared with those derived by means of the classical modal analysis [14]. The latter represents the total deflection,

$$w(x,t) = \sum_{n=1}^{\infty} Y_n(t)\,\boldsymbol{\Phi}_n(x), \tag{30}$$

where the modal coefficients of a viscously damped beam are of the form (compare [22])

$$Y_n(t) = \exp(-\zeta_n\omega_n t)\left[\left(\cos\omega_{dn}t+\frac{\omega_n}{\omega_{dn}}\zeta_n\sin\omega_{dn}t\right)Y_n(0)+\frac{1}{\omega_{dn}}\sin\omega_{dn}t\,\dot{Y}_n(0)\right] + \frac{1}{\omega_{dn}}\int_0^t P_n(\tau)\exp[-\zeta_n\omega_n(t-\tau)]\sin[\omega_{dn}(t-\tau)]\,d\tau. \tag{31}$$

5.1 *Sinusoidal force excitation*

In a first example, a spatial uniformly distributed time-harmonic force excitation, $q(x,t) = q_0 \sin \nu t$, is switched on at time $t = 0$. Viscous damping is neglected. In that particular case, the quasistatic deflection reads

$$w_S(x,t) = \frac{q_0 l^4 \sin\nu t}{24EJ_\infty}\left(1-\frac{x}{l}\right)\frac{x}{l}\left[1+\left(1-\frac{x}{l}\right)\frac{x}{l}\right] + \frac{q_0\sin\nu t}{\alpha^2}\left(\frac{1}{EJ_0}-\frac{1}{EJ_\infty}\right)\left\{\frac{1}{\alpha^2}\left[\frac{\sinh\alpha x-\sinh\alpha(x-l)}{\sinh\alpha l}-1\right]+\frac{x}{2}(l-x)\right\}. \tag{32}$$

The corresponding quasistatic internal actions are given by Eqs. (10), when substituting w_S for w and its derivatives.

The dynamic analysis according to Eqs. (15.2), (21), and (25) renders the complementary dynamic quantities:

$$w_D(x,t) = \sum_{n=1,3,5,\ldots}^{\infty} \frac{q_0 \mathscr{L}_n^{\,D}}{\mu\omega_n^{\,3}}\sin\frac{n\pi x}{l}f_n(t), \tag{33}$$

$$M_D(x,t) = \sum_{n=1,3,5,\ldots}^{\infty} \frac{q_0 EJ_\infty \mathscr{L}_n^D}{\mu\omega_n^3}\left(\frac{n\pi}{l}\right)^2\left[1+\frac{1}{\alpha^2}\left(\frac{n\pi}{l}\right)^2\right]\sin\frac{n\pi x}{l}f_n(t), \tag{34}$$

$$N_{1D}(x,t) = -\frac{1}{r}\sum_{n=1,3,5,\ldots}^{\infty} \frac{q_0 \mathscr{L}_n^D}{\mu\omega_n^3}\left[EJ_\infty - EJ_0 + \frac{EJ_\infty}{\alpha^2}\left(\frac{n\pi}{l}\right)^2\right]\left(\frac{n\pi}{l}\right)^2\sin\frac{n\pi x}{l}f_n(t), \tag{35}$$

$$Q_D(x,t) = \sum_{n=1,3,5,\ldots}^{\infty} \frac{q_0 EJ_\infty \mathscr{L}_n^D}{\mu\omega_n^3}\left(\frac{n\pi}{l}\right)^3\left[1+\frac{1}{\alpha^2}\left(\frac{n\pi}{l}\right)^2\right]\cos\frac{n\pi x}{l}f_n(t), \tag{36}$$

$$T_D(x,t) = \frac{1}{r}\sum_{n=1,3,5,\ldots}^{\infty} \frac{q_0 \mathscr{L}_n^D}{\mu\omega_n^3}\left[EJ_\infty - EJ_0 + \frac{EJ_\infty}{\alpha^2}\left(\frac{n\pi}{l}\right)^2\right]\left(\frac{n\pi}{l}\right)^3\cos\frac{n\pi x}{l}f_n(t). \tag{37}$$

$\mathscr{L}_n^D$ is the n-th complementary dynamic participation factor due to a uniformly distributed loading function,

$$\mathscr{L}_n^D = \frac{4v^2}{n\pi}, \tag{38}$$

and $f_n(t)$ denotes the n-th unit response due to a sinusoidal force excitation,

$$f_n(t) = \frac{1}{v^2-\omega_n^2}(v\sin\omega_n t - \omega_n \sin vt). \tag{39}$$

Contrary, the results according to the classical modal analysis, Eqs. (30), (31), become:

$$w(x,t) = \sum_{n=1,3,5,\ldots}^{\infty} \frac{q_0 \mathscr{L}_n}{\mu\omega_n}\sin\frac{n\pi x}{l}f_n(t), \tag{40}$$

$$M(x,t) = \sum_{n=1,3,5,\ldots}^{\infty} \frac{q_0 EJ_\infty \mathscr{L}_n}{\mu\omega_n}\left(\frac{n\pi}{l}\right)^2\left[1+\frac{1}{\alpha^2}\left(\frac{n\pi}{l}\right)^2\right]\sin\frac{n\pi x}{l}f_n(t) - \frac{q_0 EJ_\infty}{\alpha^2 EJ_0}, \tag{41}$$

$$N_1(x,t) = -\frac{1}{r}\left\{\sum_{n=1,3,5,\ldots}^{\infty} \frac{q_0 \mathscr{L}_n}{\mu\omega_n}\left[EJ_\infty - EJ_0 + \frac{EJ_\infty}{\alpha^2}\left(\frac{n\pi}{l}\right)^2\right]\left(\frac{n\pi}{l}\right)^2\sin\frac{n\pi x}{l}f_n(t) - \frac{q_0 EJ_\infty}{\alpha^2 EJ_0}\right\}, \tag{42}$$

$$Q(x,t) = \sum_{n=1,3,5,\ldots}^{\infty} \frac{q_0 EJ_\infty \mathscr{L}_n}{\mu\omega_n}\left(\frac{n\pi}{l}\right)^3\left[1+\frac{1}{\alpha^2}\left(\frac{n\pi}{l}\right)^2\right]\cos\frac{n\pi x}{l}f_n(t), \tag{43}$$

$$T(x,t) = \frac{1}{r}\sum_{n=1,3,5,\ldots}^{\infty} \frac{q_0 \mathscr{L}_n}{\mu\omega_n}\left[EJ_\infty - EJ_0 + \frac{EJ_\infty}{\alpha^2}\left(\frac{n\pi}{l}\right)^2\right]\left(\frac{n\pi}{l}\right)^3\cos\frac{n\pi x}{l}f_n(t), \tag{44}$$

with

$$\mathscr{L}_n = \frac{4}{n\pi}. \tag{45}$$

It is noted that the series solutions Eqs. (40)–(42) are slowly convergent compared to the corresponding complementary dynamic series Eqs. (33)–(35). The total shear and slip forces given by Eqs. (43), (44) are even divergent, whereas the expansions Eqs. (36), (37) converge.

5.2 Random force excitation

In a further example, a spatially uniformly distributed load $q = q_0 f(t)$, see Fig. 2, with time evolution $f(t)$, is switched on at time $t = 0$. Figure 3 shows $f(t)$ chosen in this example, that corresponds to one sample of a band-limited Gaussian white noise process with

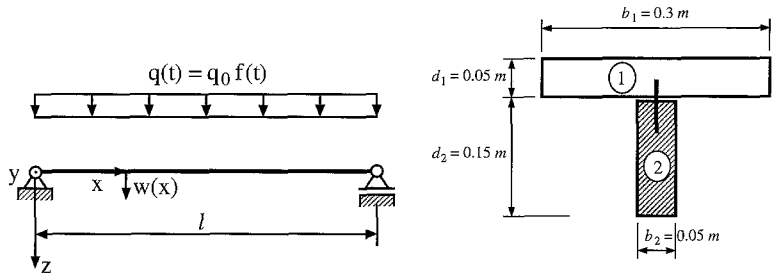

Fig. 2. Simply supported single-span beam; dimensions of the cross-section

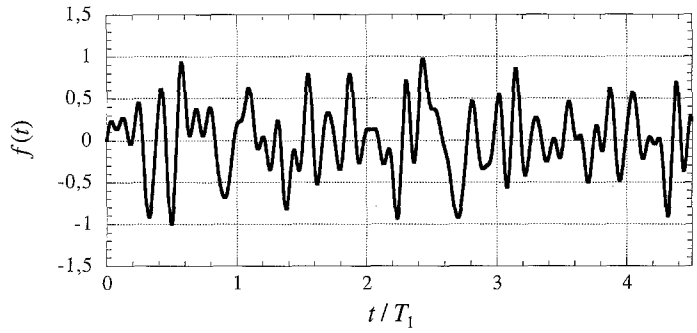

Fig. 3. Time evolution corresponding to one sample of a band-limited Gaussian white noise process with $30 \leq \omega \leq 500$ *rad/s*

$30 \leq \omega \leq 500$ *rad/s*. Duhamel's integral equation (23) is solved numerically using the procedure proposed in Appendix A. In all subsequent calculations, the geometrical and mechanical properties of the two-layer beam are characterized by the following parameters: $l = 4\ m$, $b_1 = 0.3\ m$, $d_1 = 0.05\ m$, $b_2 = 0.05\ m$, $d_2 = 0.15\ m$, $q_0 = 486\ N/m$, $E_1 = 12000\ MN/m^2$, $E_2 = 8000\ MN/m^2$, $k = 50\ MN/m^2$, $\varrho_1 = 2500\ kg/m^3$, $\varrho_2 = 800\ kg/m^3$. The damping coefficients are assumed to be constant for all modes: $\zeta_i = 0.09$, $i = 1, \ldots, N$.

In Table 1, the first nine eigenfrequencies of layered beams with various interlaminar connection conditions are arranged. It turns out that in the higher frequency range the eigenvalues of the elastically bonded beam converge towards those of the beam without layer connection.

Table 1. Eigenfrequencies of simply supported two-layer beams with various interlaminar connection conditions

Eigenfrequency	Elastic bond [rad/s]	Perfect bond [rad/s]	Without bond [rad/s]
1	61.99	72.44	36.22
2	201.37	289.78	144.89
3	399.31	652.01	326.00
4	661.71	1159.13	579.56
5	992.67	1811.14	905.57
6	1394.11	2608.03	1304.02
7	1866.93	3549.83	1774.91
8	2411.57	4636.51	2318.25
9	3028.27	5868.08	2934.04

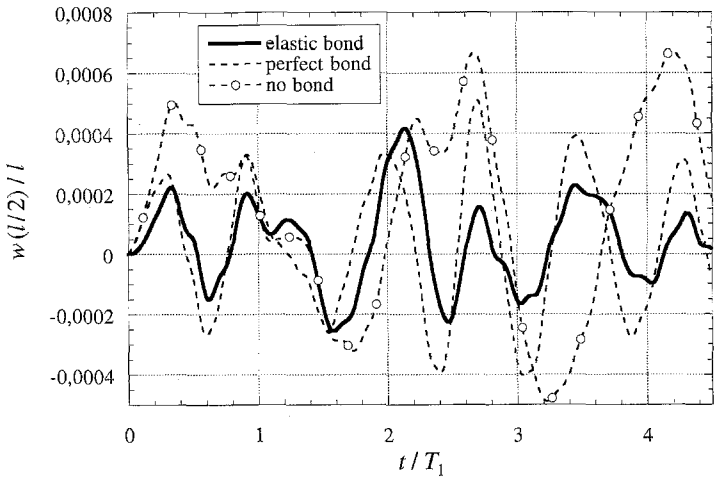

Fig. 4. Total dynamic deflection in $x = l/2$

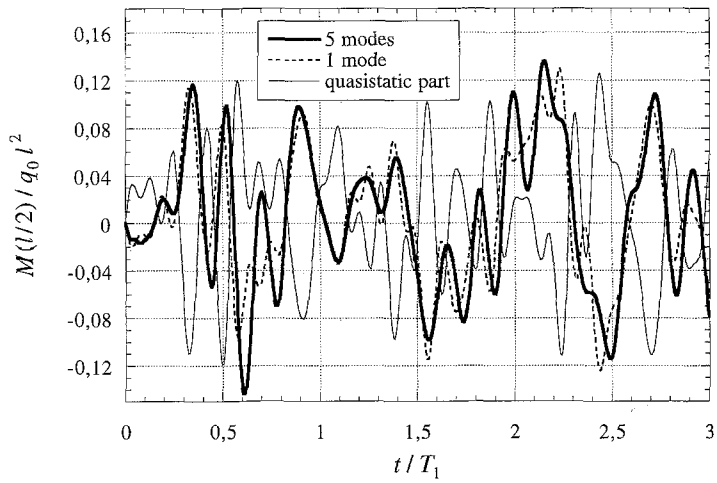

Fig. 5. Total dynamic and quasistatic bending moment in $x = l/2$

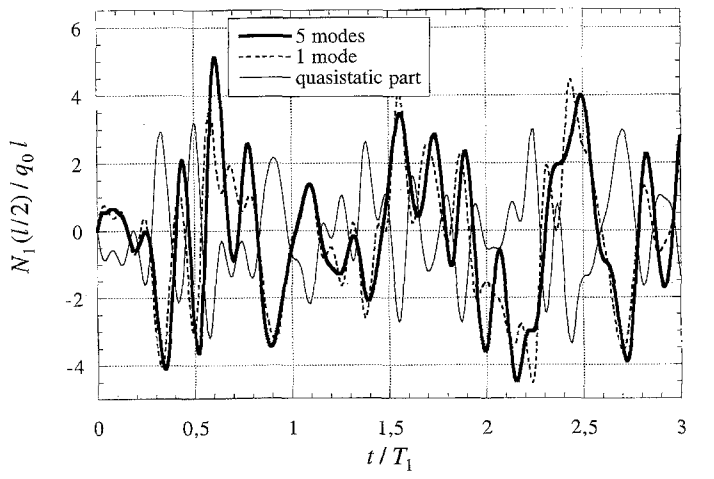

Fig. 6. Total dynamic and quasistatic axial force of the upper layer in $x = l/2$

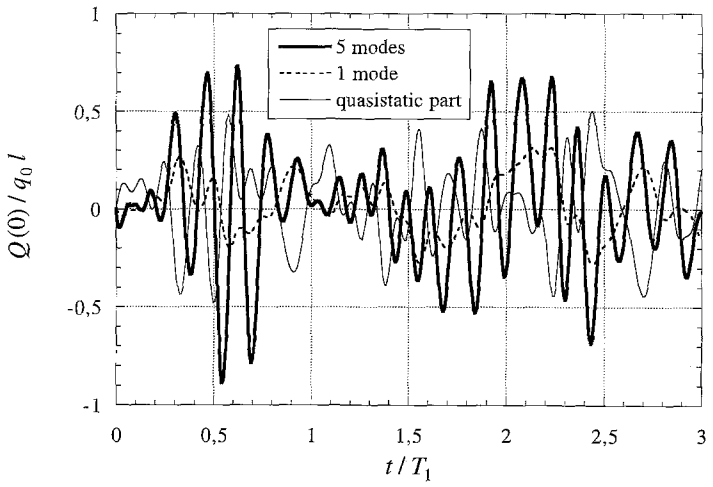

Fig. 7. Total dynamic and quasistatic lateral shear force in $x = 0$

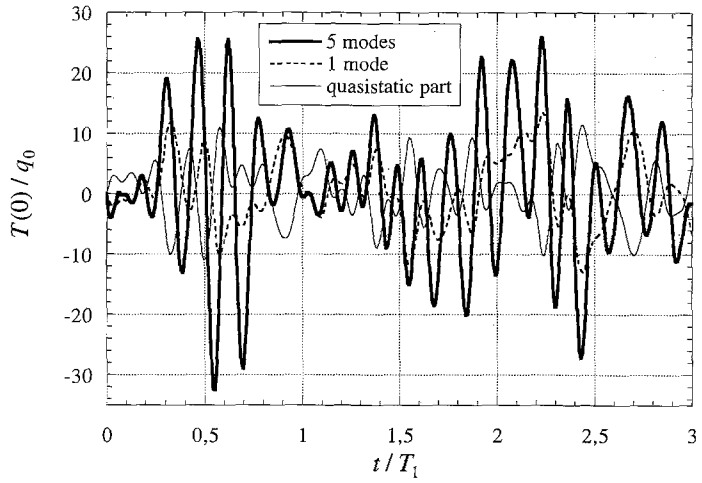

Fig. 8. Total dynamic and quasistatic shear force transmitted between the two layers in $x = 0$

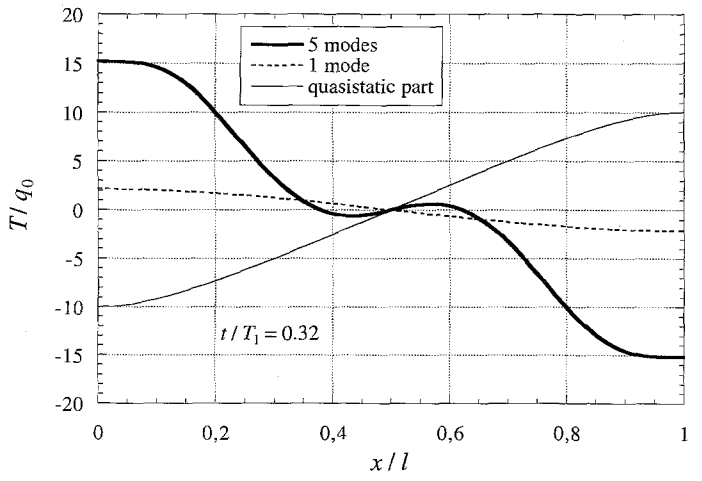

Fig. 9. Total dynamic and quasistatic spatial distribution of the shear force at time instant $t/T_1 = 0.32$

Figure 4 shows the transient deflection at midspan, with $T_1 = 2\pi/\omega_1$ denoting the fundamental vibration period. The solution of the elastically bonded beam is displayed by the full line, whereas the dashed line corresponds to the response considering rigid interconnection. The dashed line with circles illustrates the lateral displacement when no connection between the two layers is assumed. For the numerical computation, the complementary dynamic deflection is sufficiently well approximated by means of the first five symmetric modes.

Figures 5 and 6 display the evolution of the total bending moment and of the total axial force of the upper layer at midspan, respectively, as well as the corresponding (closed-form) quasistatic results. Furthermore, the approximate single-mode solution is compared to the results according to a five-mode expansion. Especially for the lateral shear force, Fig. 7, and for the shear force transmitted between the two layers, Fig. 8, the higher modes of the complementary dynamic response become dominant.

Finally, in Fig. 9 the distribution of the shear force along the beam axis at a certain time instant, $t/T_1 = 0.32$, is illustrated.

6 Conclusions

The initial-boundary value problem of flexural vibrations of elastic two-layer beams with interlayer slip is solved. The Bernoulli-Euler hypothesis is assumed to hold for each layer separately, and a linear constitutive equation between the horizontal slip and the interlaminar shear force is taken into account. The solution of the corresponding partial equation of motion is found by separating the response of the beam in a quasistatic and in a complementary dynamic part. The quasistatic portion that probably contains singularities can be represented in a closed form. The remaining non-singular complementary dynamic part is approximated by a truncated modal series of fast accelerated convergence. Light damping is considered by means of modal damping coefficients, and the solution of the resulting generalized decoupled single-degree-of-freedom oscillators is given by Duhamel's convolution integral. Numerical examples are given for simply supported composite beams under harmonic and random excitations. The computational procedure described in detail shows high improvement when compared to the classical modal analysis approach.

Appendix A

Numerical evaluation of the dynamic response

In case of a lateral loading function with arbitrary time history, the solution is found incrementally. The convolution integral equation (23) is evaluated by assuming a linear variation of the load variable q within the time increment $\Delta t = t_{a+1} - t_a$,

$$q(x,t) = q(x,t_a) + \Delta q(x)\, g(\bar{t}), \qquad \bar{t} = t - t_a, \tag{A1}$$

$$g(\bar{t}) = 1, \quad \bar{t} \geq \Delta t; \qquad g(\bar{t}) = \bar{t}/\Delta t, \quad 0 \leq \bar{t} \leq \Delta t; \qquad g(\bar{t}) = 0, \quad \bar{t} \leq 0. \tag{A2}$$

Discretization of the incremental load variables by application of higher-order spline functions is discussed in [26]. In the following, subscripts $(.)_a$ and $(.)_{a+1}$ refer to variables at the beginning and at the end of the time step, respectively. When computing the dynamical modal response according to Eq. (23), the time derivatives $\dot{g}$ and $\ddot{g}$ enter, and, hence the approximate variation of

$g(\bar{t})$ within the time interval must have unique first and second derivatives at t_a and t_{a+1}. This degree of smoothness is achieved by assuming at least the linear ramp function $g(\bar{t})$ to start at t_a^- immediately after t_a, and to end at t_{a+1}^- immediately before t_{a+1}. Accordingly, the first and the second derivative of Δq become

$$\Delta\dot{q} = \Delta q(x)/\Delta t, \qquad \Delta\ddot{q} = \Delta q(x)\,[\delta(0) - \delta(\Delta t)]/\Delta t, \tag{A3}$$

with Dirac delta function δ. The evaluation of Eq. (23) together with Eq. (A3) renders the increments of the complementary dynamic coefficients ([22]),

$$\Delta Y_n^D = \dot{\mathscr{I}}_n Y_n^D(t_a) + \mathscr{I}_n \dot{Y}_n^D(t_a) - \frac{1}{\omega_n^2}\mathscr{D}_n \Delta P_n, \tag{A4}$$

with the following abbreviations:

$$\dot{\mathscr{I}}_n = \exp(-\zeta_n\omega_n\Delta t)\left[\cos\omega_{dn}\Delta t + \frac{\omega_n}{\omega_{dn}}\zeta_n \sin\omega_{dn}\Delta t\right] - 1, \tag{A5}$$

$$\mathscr{I}_n = \frac{1}{\omega_{dn}}\exp(-\zeta_n\omega_n\Delta t)\sin\omega_{dn}\Delta t, \tag{A6}$$

$$\mathscr{D}_n = \frac{1}{\omega_n}\frac{1}{\Delta t}\left\{2\zeta_n + \exp(-\zeta_n\omega_n\Delta t)\left[\frac{\omega_n}{\omega_{dn}}\sin\omega_{dn}\Delta t(1 - 2\zeta_n^2) - 2\zeta_n\cos\omega_{dn}\Delta t\right]\right\}. \tag{A7}$$

ΔP_n stands for the increment of the generalized load, compare [22],

$$\Delta P_n = \int_0^l \Delta q\left[\frac{\alpha^2}{EJ_\infty}\boldsymbol{\Phi}_n - \frac{1}{EJ_0}\boldsymbol{\Phi}_{n,\xi\xi}\right]d\xi + \sum_{j=1}^{2}\boldsymbol{C}_j[\Delta q(0,l)]\,\boldsymbol{\Phi}_n(0,l). \tag{A8}$$

Relation (A4) has to be completed by the increments of the velocity of modal coefficients. They are given by ([22])

$$\Delta\dot{Y}_n^D = \dot{\mathscr{I}}_n Y_n^D(t_a) + \mathscr{I}_n \dot{Y}_n^D(t_a) - \frac{1}{\omega_n^2}\dot{\mathscr{D}}_n \Delta P_n, \tag{A9}$$

with

$$\dot{\mathscr{I}}_n = \exp(-\zeta_n\omega_n\Delta t)\left(-\frac{\omega_n^2}{\omega_{dn}}\zeta_n^2 - \omega_{dn}\right)\sin\omega_{dn}\Delta t, \tag{A10}$$

$$\mathscr{I}_n = \left[\cos\omega_{dn}\Delta t - \frac{\omega_n}{\omega_{dn}}\zeta_n\sin\omega_{dn}\Delta t\right]\exp(-\zeta_n\omega_n\Delta t) - 1, \tag{A11}$$

$$\dot{\mathscr{D}} = \frac{1}{\Delta t}[\exp(-\zeta_n\omega_n\Delta t)(\cos\omega_{dn}\Delta t + b_n\sin\omega_{dn}\Delta t) - 1], \tag{A12}$$

and

$$b_n = \zeta_n\left[2\frac{\omega_{dn}}{\omega_n} - \frac{\omega_n}{\omega_{dn}}(1 - 2\zeta_n^2)\right]. \tag{A13}$$

Adding the exactly computed quasistatic deflection increments to the complementary dynamic increments leads to the total flexural response,

$$\Delta w(x) = \Delta w^S(x) + \sum_{n=1}^{N}\boldsymbol{\Phi}_n(x)\,\Delta Y_n^D, \tag{A14}$$

whereby the infinite series are approximated by a finite number of N modes.

Referenes

[1] Vinson, J. R., Sierakowski, R. L.: The behavior of structures composed of composite materials. Amsterdam: Martinus Nijhoff 1987.
[2] Reddy, J. N.: An evaluation of equivalent-single-layer and layerwise theories of composite laminates. Comp. Struct. **26,** 21–35 (1993).
[3] Yu, Y.-Y.: A new theory of elastic sandwich plates-one-dimensional case. J. Appl. Mech. **26,** 415–421 (1959).
[4] Swift, G. W., Heller, R. A.: Layered beam analysis. J. Eng. Mech. Div., ASCE **100,** 267–282 (1974).
[5] Heuer, R.: Static and dynamic analysis of transversely isotropic, moderately thick sandwich beams by analogy. Acta Mech. **91,** 1–9 (1992).
[6] Whitney, J. M., Pagano, N. J.: Shear deformation in heterogeneous anisotropic plates. J. Appl. Mech. **37,** 1031–1036 (1970).
[7] Reddy, J. N.: A simple higher-order theory for laminated composite plates. J. Appl. Mech. **51,** 745–752 (1984).
[8] Homberg, H.: Brücke mit elastischem Verbund zwischen Stahlhauptträger und der Betonfahrbahntafel. Bauingenieur **27,** 213–216 (1952).
[9] Hoischen, A.: Verbundträger mit elastischer und unterbrochener Verdübelung. Bauingenieur **29,** 241–244 (1954).
[10] Pischl, R.: Ein Beitrag zur Berechnung hölzener Biegeträger. Bauingenieur **43,** 448–451 (1968).
[11] Goodman, J. R., Popov, E. P.: Layered beam systems with interlayer slip. J. Struct. Div., ASCE **94,** 2535–2547 (1968).
[12] Girhammar, U. A., Gopu, V. K. A.: Composite beam – columns with interlayer slip-exact analysis. J. Struct. Eng. **119,** 1265–1282 (1993).
[13] Mistakis, E. S., Thomopoulos, K., Avdelas, A., Panagiotopoulos, P. D.: On the nonmonotone slip effect in the shear connectors of composite beams. Int. J. Eng. Anal. Des. **1,** 395–409 (1994).
[14] Girhammar, U. A., Pan, D.: Dynamic analysis of composite members with interlayer slip. Int. J. Solids Struct. **30,** 797–823 (1993).
[15] Boley, B. A., Barber, A. D.: Dynamic response of beams and plates to rapid heating. J. Appl. Mech. **24,** 413–416 (1957).
[16] Ziegler, F., Irschik, H.: Dynamic analysis of elastic plastic beams by means of thermoelastic solutions. Int. J. Solids Struct. **21,** 819–829 (1985).
[17] Fotiu, P. A., Irschik, H., Ziegler, F.: Modal analysis of elastic-plastic plate vibrations by integral equations. EABE **14,** 81–97 (1994).
[18] Adam, C., Ziegler, F.: Forced flexural vibrations of elastic-plastic composite beams with thick layers. Comp. Part B **28B,** 201–213 (1997).
[19] Irschik, H., Ziegler, F.: Dynamics of linear elastic structures with selfstress: a unified treatment for linear and nonlinear problems. ZAMM **68,** 199–205 (1988).
[20] Ziegler, F.: Developments in structural dynamic viscoplasticity including ductile damage. ZAMM **72,** T5–T15 (1992).
[21] Irschik, H., Ziegler, F.: Dynamic processes in structural thermo-viscoplasticity. AMR **48,** 301–316 (1995).
[22] Jeschko, A.: Biegeschwingungen zweischichtiger elastischer Balken mit nachgiebigem Verbund – ein analytisches Lösungsverfahren. Master's Thesis, Technical University of Vienna, Dept. of Civil Eng., Vienna 1996.
[23] Weaver, W., Timoshenko, S., Young, D. H.: Vibration problems in engineering, 5th ed. New York: Wiley 1990.
[24] Clough, R. W., Penzien, J.: Dynamics of structures, 2th ed. New York: McGraw-Hill 1993.
[25] Ziegler, F.: Mechanics of solids and fluids, 2nd ed. New York: Springer 1995.
[26] Holl, H. J.: Ein effizienter Algorithmus für nichtlineare Probleme der Strukturdynamik mit Anwendung in der Rotordynamik. Doctoral Thesis, University of Linz, Linz 1995.

Authors' addresses: C. Adam and R. Heuer, Institut für Allgemeine Mechanik, Technische Universität Wien, Wiedner Hauptstraße 8–10/E201, A-1040 Wien; A. Jeschko, Stuwerstraße 6/20, A-1020 Wien, Austria